Journal of Photochemistry and Photobiology A: Chemistry 219 (2011) 109–114

Contents lists available at ScienceDirect

Journal of Photochemistry and Photobiology A: Chemistry

journal homepage: www.elsevier.com/locate/jphotochem

Laser photodeposition of sulfur and room-temperature solid-state reaction with copper

J. Pola [a,*], M. Urbanová [a], D. Pokorná [a], Z. Bastl [b], S. Bakardjieva [c], J. Šubrt [c], P. Bezdička [c]

[a] Laboratory of Laser Chemistry, Institute of Chemical Process Fundamentals, ASCR, Rozvojova Str. 135, 16502 Prague, Czech Republic
[b] J. Heyrovský Institute of Physical Chemistry, ASCR, 18223 Prague, Czech Republic
[c] Institute of Inorganic Chemistry, ASCR, 25068 Řež, Czech Republic

ARTICLE INFO

Article history:
Received 24 October 2010
Received in revised form 26 January 2011
Accepted 27 January 2011
Available online 3 February 2011

Keywords:
Photodeposition of sulfur
Solid-state reaction
Copper
Sulfur
CuS and Cu_2S nanograins
Growth of a-CuS/Cu_2S structures

ABSTRACT

Ultraviolet laser photolysis of thiirane (C_4H_2S) allows chemical vapor deposition of sulfur-containing solid which undergoes room-temperature reaction with copper and yields sub-μm-sized amorphous filamentary CuS/Cu_2S/C/H structures incorporating CuS and Cu_2S nanograins. Properties of these structures were examined by Fourier transform infrared, Raman and X-ray photoelectron spectroscopies, X-ray diffraction and by electron microscopy. The results demonstrate the occurrence of reaction between solid sulfidizing reagent and copper at room temperature.

1. Introduction

Copper sulfides have arrested a lot of attention due to their applications in solar cells, electroconducting electrodes, optical filters, superionic materials and chemical sensors (e.g. [1–6]). These binary compounds occur in a variety of compositions and morphologies [7] and their thin films and nanoparticles were prepared by a number of techniques in the gaseous, liquid and solid phase. These techniques involve *reactive sputtering* in H_2S [8,9], *gas-phase deposition* from H_2S and Cu dithiocarbamate or diketonate [10,11], *room-temperature gas–solid reaction* between H_2S/O_2 and Cu [12,13], *high-temperature gas–solid reactions* between Cu or CuCl and H_2S [14,15] and between CuCl and Si and gaseous sulfur [16], *solid–liquid reaction* between sulfur dissolved in amine and Cu [17], CuO(s) and thiourea solution [18], S(s)–Cu diketonate solution [5] and $CuCl_2/Na_2S$-liquid surfactant [19], and many *inorganic reactions in solution* as solvothermal (e.g. [5,6,20–23]), hydrothermal (e.g. [24,25]), microwave-induced solvothermal [26], spray-pyrolytic (e.g. [27,28]), ionic liquid-assisted [29], ionic layer adsorption [30] chemical bath and [31] and microwave assisted chemical bath [32,33] reactions.

Traditional and simple synthesis of copper sulfides from the elements is feasible only at high temperatures (e.g. [34,35]) and the direct reaction at temperatures below 150 °C is restricted by the passivation effect of the CuS_x layer on copper surface and its completion requires reactant milling [36] or the use of solvent [37,38]. As for the room-temperature reaction between sulfur and copper, it has been only reported for sulfur vapor and revealed as extremely slow and resulting in thin Cu_2S overgrowth on Cu with sulfur vapor exposures of the order of 10^{-7} Torr h [39].

We have previously reported on UV laser gas-phase photolysis of organic selenides [40,41] for photochemical deposition of selenium films on different metal substrates and found out that thin solid Se films undergo fast room-temperature solid-state reaction with copper and other metals substrates [42].

It was of our further interest to examine the feasibility of the yet unobserved room-temperature reaction between Cu and solid photochemically deposited sulfur. Here we report on UV laser photolysis of thiirane (C_4H_2S) and reveal that this reaction allows deposition of sulfur containing solid which rapidly reacts with copper at room temperature to yield copper sulfides. We also show that this reaction allows fast formation of sub-μm-sized amorphous copper sulfide filaments containing crystalline grains of copper sulfides.

2. Experimental

The ultraviolet (UV) laser photolysis of gaseous thiirane (30 Torr) was carried out in a Pyrex reactor (two orthogonally positioned tubes, one fitted with two KBr windows and the other

* Corresponding author. Tel.: +420 2 20390308; fax: +420 2 20920661.
E-mail address: pola@icpf.cas.cz (J. Pola).

1010-6030/$ – see front matter © 2011 Elsevier B.V. All rights reserved.
doi:10.1016/j.jphotochem.2011.01.024

furnished with two quartz plates, 140 ml in volume, base pressure less than 0.05 Torr) using an ArF (ELI 94) laser operating at 193 nm with a pulse energy of 50 mJ and repetition rate of 10 Hz. The reactor was equipped with a sleeve with a rubber septum and PTFE valve connecting to a vacuum manifold. It accommodated a 1 cm^2-sized copper substrate or a tungsten substrate (as an inert standard) which were covered with the deposit in the course of the photolysis and transferred after thorough evacuation for examination of spectral, diffraction and microscopic properties.

In a typical experiment ca. 60% decomposition of thiirane was accomplished in 7 min-irradiation as checked by in situ Fourier transform infrared (FTIR) spectral analysis using analytical band of thiirane at 627 cm^{-1}. Aliquots of the irradiated reactor content were sampled by a gastight syringe (Dynatech Precision Sampling) and analyzed by gas-chromatography–mass spectroscopy (GC–MS) (a Shimadzu QP 5050 mass spectrometer, 60 m capillary column Neutrabond-1, programmed temperature 30–200 °C). The decomposition products were identified through their FTIR diagnostic bands (an FTIR spectrometer (Nicolet Impact), ethene 949 cm^{-1}, ethyne 730 cm^{-1} and CS_2 1539 cm^{-1}) and through mass spectra using the NIST library. The same GC–MS analysis was also applied to solution of the deposit in CS_2.

The deposited films were after evacuation of the gaseous products analyzed with a Raman spectrometer (Nicolet Almega XR, resolution 2 cm^{-1}, excitation wavelength 473 nm and power 10 mW), X-ray photoelectron spectroscopy, X-ray diffraction and by electron microscopy.

The Raman spectral analysis was carried out on different microregions of the films to examine the deposited films for non-homogeneous spots. Diffraction patterns were measured with an X-ray diffractometer (PANalytical X'Pert PRO) equipped with a conventional X-ray tube (Co Kα radiation, 40 kV, 30 mA, point focus), an X-ray monocapillary with diameter of 0.1 mm, and a multichannel detector X'Celerator with an anti-scatter shield.

Scanning electron microscopy (SEM) images were obtained with a microscope (Philips XL30 CP) equipped with an energy-dispersive analyzer (EDAX DX-4) of X-ray radiation. Transmission electron microscopy (TEM) analysis (particle size and phase analysis) was carried out with a microscope (JEOL JEM 3010) operating at 300 kV and equipped with an EDS detector (INCA/Oxford) and CCD Gatan (Digital Micrograph software) on scraped samples that were subsequently dispersed in ethanol followed by application of a drop of a diluted suspension on a Ni grid.

The C 1s, S $2p_{3/2}$ and Cu $2p_{3/2}$ photoelectron spectra of the deposited films were measured in an ESCA 310 electron spectrometer (Scienta) with a base pressure better than 10^{-9} Torr using Al Kα radiation (1486.6 eV) for electron excitation. The surface composition of the deposited film was determined by correcting the spectral intensities for subshell photoionization cross-sections [43].

Copper sheets (Lachema, 99.9% purity) were scrubbed to remove superficial oxide layers and thiirane (Aldrich, purity 98%) was distilled on the vacuum line prior to use.

3. Results and discussion

The ArF laser photolysis of gaseous thiirane (30 Torr) with laser beam parallel to Cu surface results in the formation of ethene (a main product), small amounts of ethyne, hydrogen sulfide and carbon disulfide, and traces of methane, propene, methylthiirane and ethanethiol (Fig. 1).

The observed formation of ethene, ethyne and hydrogen sulfide is compatible [44–46] with primary channels yielding S + C_2H_4, HS + C_2H_3, and H + SC_2H_3 and with secondary cleavages of HS and SC_2H_3 species, all of which contributing to formation of sulfur atoms. We assume that concomitantly with these channels, S atoms

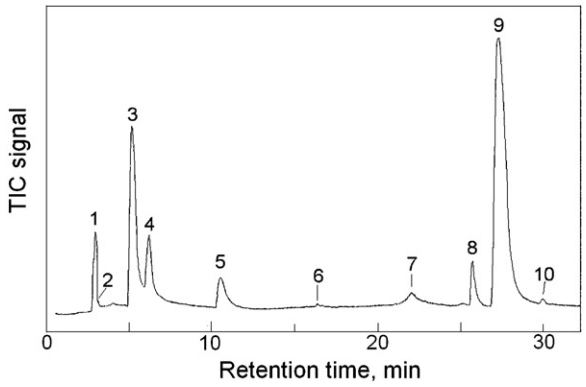

Fig. 1. GC–MS trace of volatile products of ArF laser photolysis of thiirane. *Designation:* 1, air; 2, methane; 3, ethene; 4, ethyne; 5, H_2S; 6, propene; 7, CH_3SH; 8, carbon disulfide; 9, thiirane; 10, methylthiirane.

are also formed by photolysis of CS_2 which is produced in molar amounts 2.3 times lower than C_2H_4. The photolysis of CS_2 is known to take place as the dissociation into CS + S and result in deposition of elemental sulfur and polythiene $(CS)_n$ [47]. The observed volatile products and the previously determined primary steps in the gas-phase photolysis of thiirane are thus compatible with gas-phase deposition of sulfur as a major and polythiene as a minor solid product.

Copper substrate becomes black immediately after the photolysis, which confirms that the depositing solid reacts rapidly with Cu surface. The Raman spectra of the black layer on Cu measured after 2 h evacuation of the reactor were compared to those of the deposit on tungsten (Fig. 2) and they show the presence of copper sulfide and a C/H/S polymer.

The spectra of the deposit on tungsten (Fig. 2a) consist of a strong band centered at 470 cm^{-1}, medium bands at 221 and 153 cm^{-1} and weak bands at 830–870 cm^{-1}, 1440 cm^{-1} and 2910 cm^{-1}. The bands at 470, 221 and 153 cm^{-1} belong to elemental sulfur, specifically to cyclooctasulfur S_8 [48], and the bands at 830–870, 1440 and 2910 cm^{-1} correspond, in the given order, to –C=S– stretches, a C=C stretch in $(S_2)C=C(S_2)$ configuration and to two-photon-excited scattering and/or a C–H stretching mode [47]. The spectra of the deposit on copper (Fig. 2b) show a strong band at 472 cm^{-1} along with weak bands at 266 and 910 cm^{-1}, which are assignable to copper sulfide and coincide with the scattering pattern of annealed CuS [49]. The medium band at 1446 cm^{-1} and the week band at 2885 cm^{-1} (seen also in the spectrum on tungsten, Fig. 2a) assign to the vibrations of the C/H/S polymer.

The X-ray photoelectron spectra of the superficial layers of the deposit on Cu show the presence of sulfur, copper, carbon and small

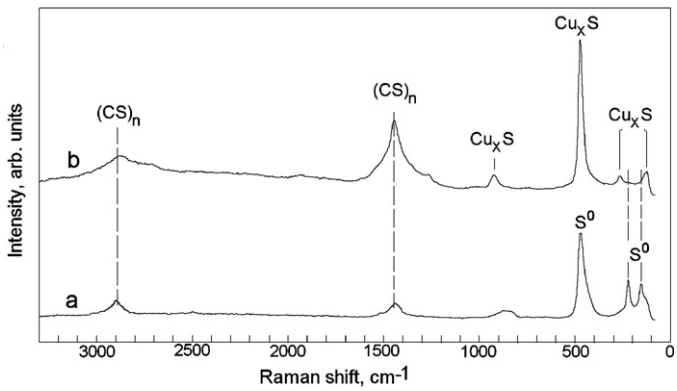

Fig. 2. Raman spectra of the deposit on W (a) and Cu (b) substrates.

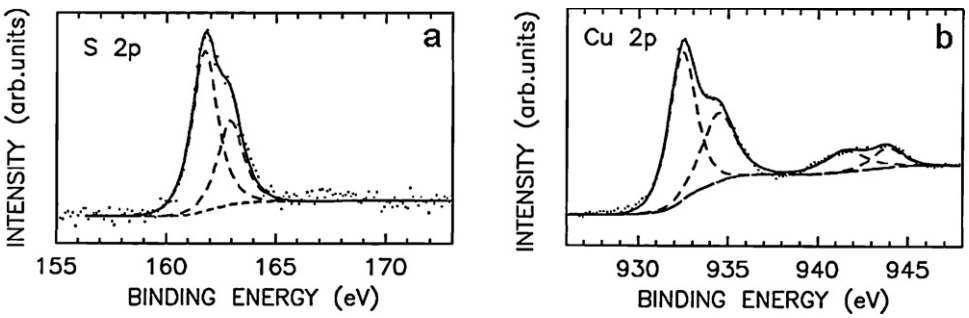

Fig. 3. Spectrum of S 2p (a) and Cu $2p_{3/2}$ (b) photoelectrons of the deposit on Cu substrate.

amounts of oxygen. The S/Cu atomic ratio ~0.4 and the S $2p_{3/2}$ signal (binding energy 161.7 eV) along with the Cu $2p_{3/2}$ spectrum (components at 932.4 and 934.4 eV) correspond [50] to sulfidic (S^{2-}) sulfur and to a mixture of 65% of Cu_2S and 35% of CuS (Fig. 3). The assignment of Cu_2S is in accord with the determined value of kinetic energy of the Auger $L_3M_{45}M_{45}(^1G)$ electrons 917.3 eV. Some samples also show small contributions of the S $2p_{3/2}$ signal at 164.0 eV and confirm [51] that the sulfidic sulfur is accompanied with –C–S–C-moieties and/or elemental sulfur.

The Fourier transform infrared spectrum of the deposit (Fig. 4) shows absorption bands at 2962, 2912 and 2855 cm^{-1} belonging to C–H stretch, a strong band at 1640 cm^{-1} assignable to ν(C=C) vibration in conjugated systems, bands at 1535 and 1514 cm^{-1} along with bands at 1440–1370 cm^{-1} which are attributed to S-substituted C=C stretches, a band at 1251 cm^{-1} belonging to skeletal vibrations of C=C bonds, and bands at 1175 and 1050 cm^{-1} assigned to C=S stretch. The bands at 488, 470 and 430 cm^{-1} relate to S–S bridges, and particularly to stretching vibration of sulfur allotropes. We conclude that the spectral pattern includes features of polythiene [47] and elemental sulfur (S_8).

Electron microscopy analysis (Fig. 5) shows bundles of sub-μm-thick filaments which are longer than 50 μm. These filaments are ended with a wider parts consisting of agglomerated globules and resemble stamen in flowers. The energy dispersive X-ray-SEM analyses reveal atomic percentage of elements (S, 20–28%; Cu, 44–46%; C, 18–23%; O, 5–8%) and they can be accounted for by contribution of both filaments and the environment of merged particles (best seen in Fig. 5a).

The micro-X-ray diffraction analysis of the deposit (Fig. 6) carried out on several samples reveals the occurrence of an amorphous state or very low signals compatible [52] with Cu_2S digenite. These findings, along with the Raman spectral data, support the prevalence of amorphous over crystalline copper sulfide(s).

The high-resolution transmission electron microscopy (HRTEM) analysis of the deposit is compatible [52] with amorphous phase which contains crystalline nanograins of CuS, Cu_2S and carbon (Fig. 7). The identification of these Cu_xS nanograins in amorphous blend of Cu_xS and carbon phase is possible through FFT (finite Fourier transform) diffraction patterns (in insets) and

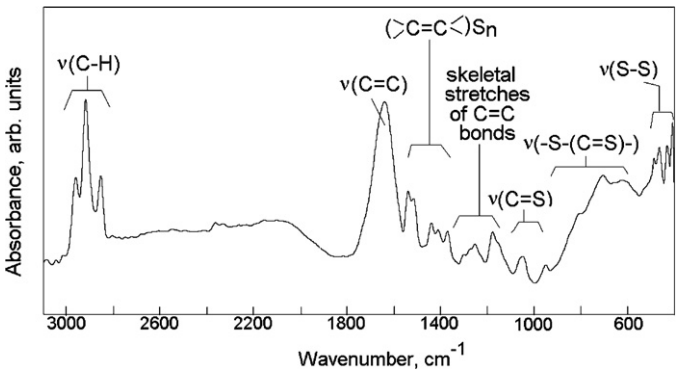

Fig. 4. FTIR spectrum of the deposit on KBr substrate.

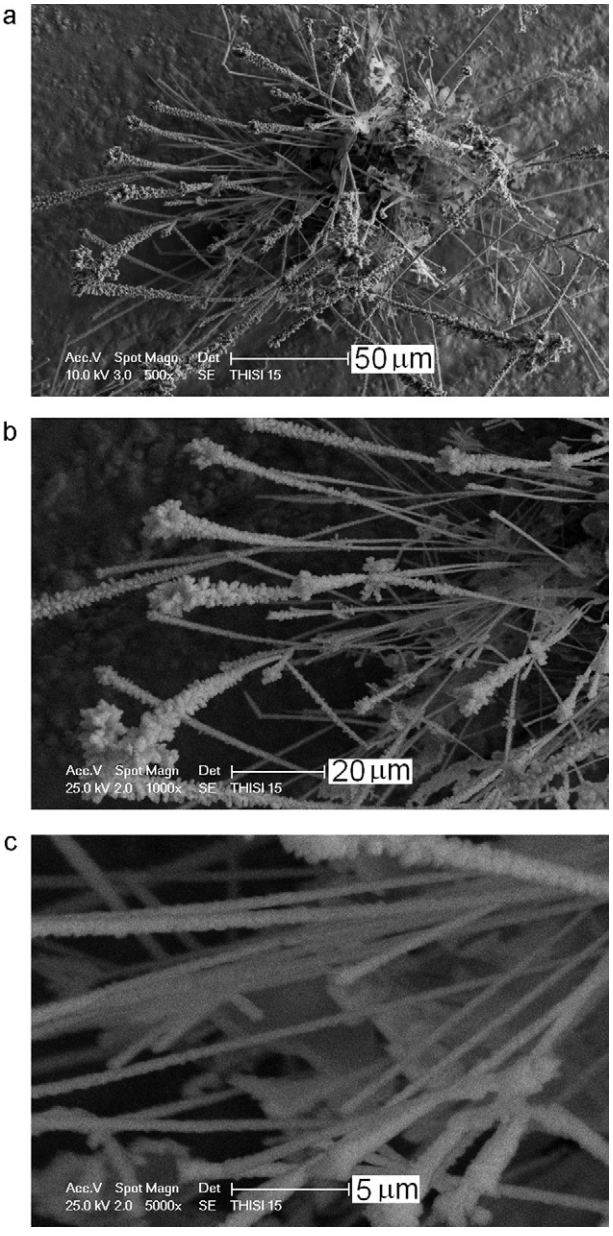

Fig. 5. SEM images of the deposit on Cu substrate showing amorphous sub-μm-sized flower-like filamentary features at different magnification (a–c).

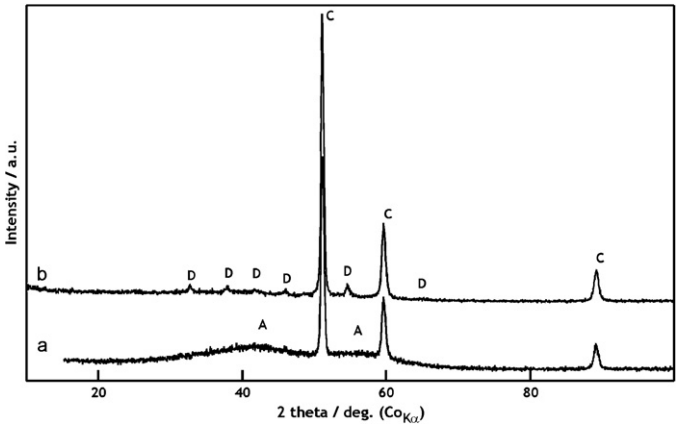

Fig. 6. Typical micro-XRD patterns of the deposit showing (a) an amorphous phase (A) and (b) very low signals of digenite (D) on copper substrate (C).

is illustrated in Figs. 7 and 8. The lattice image of hexagonal copper sulfide Cu_2S with interplanar spacing $d_{(102)}$ = 2.40 Å and $d_{(110)}$ = 1.97 Å (Fig. 7a and b) corresponds to chalcocite, PDF ICDD 24-0057. Hexagonal lattice structure *P*63/*mmc* of CuS confirmed by $d_{(102)}$ = 3.02 Å and $d_{(103)}$ = 2.76 Å (Fig. 7c and d) relates to covellite (PDF ICDD 75-2234). Both CuS and Cu_2S nanograins are in neighborhood of amorphous carbon and hexagonal carbon (interlayer spacing $d_{(110)}$ = 4.47 Å (PDF ICDD 20-0257)) (Fig. 7).

The adjacent position of two different nanocrystals is seen in Fig. 8. Two ca. 200 nm-sized bodies merging into each other (Fig. 8a) provide illustration of an amorphous nanobody (1) in contact with a nanocrystalline features-containing body (2). The energy dispersive X-ray spectroscopy analysis of the respective objects shows atomic C/S ratios 1.9/1 and 2.9/1, and the electron diffraction and HRTEM images of the nanobody 2 reveal lattice planes and interlayer spacing values of co-existing nanocrystalline grains of CuS, Cu_2S and carbon (Fig. 8b–d).

These data allow assume that both nanobodies 1 and 2 grow from the copper–sulfur inter-phase through mutual diffusion of both counterparts, which initially leads to development of Cu–S amorphous phase and in later stages to crystalline Cu–S nanophases when the proper Cu/S ratios have been attained. We presume that reduction of sulfur and oxidation of copper (leading to formation of copper sulfides) occurs during development of amorphous Cu–S phase and that the filament formation is facilitated through growth of amorphous and crystalline CuS_x in inner layers and a forced motion of polythiene component to outer layers.

All the complementary analyses are thus in agreement with a growth of amorphous sub-μm-thick and several μm-long filamentary, flower-like features that contain Cu_2S and CuS nanograins in an amorphous phase composed of Cu_xS constituent, C/H/S poly-

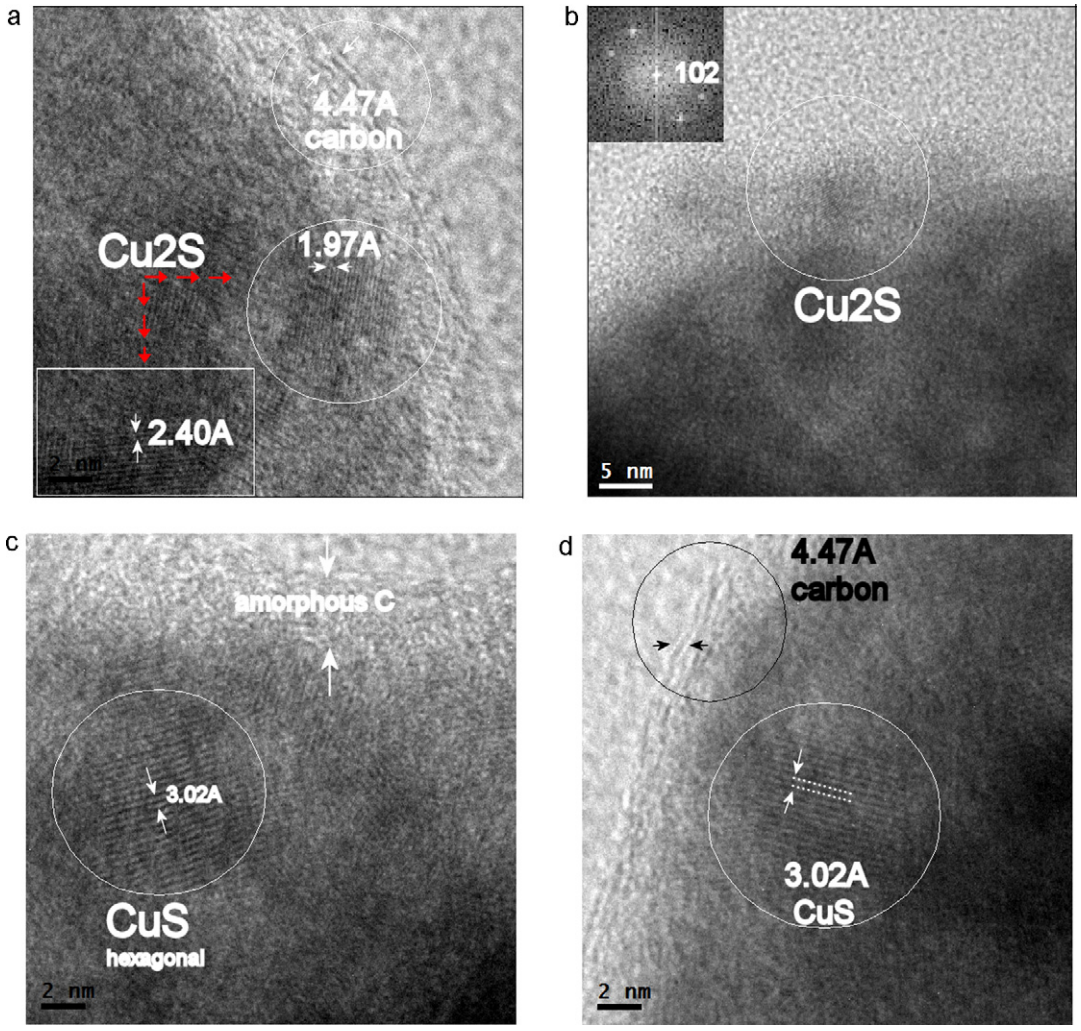

Fig. 7. HRTEM images of the deposit scraped from Cu substrate, showing nanoregions of Cu_2S (a, b) and CuS (c, d) in contact with amorphous and hexagonal carbon.

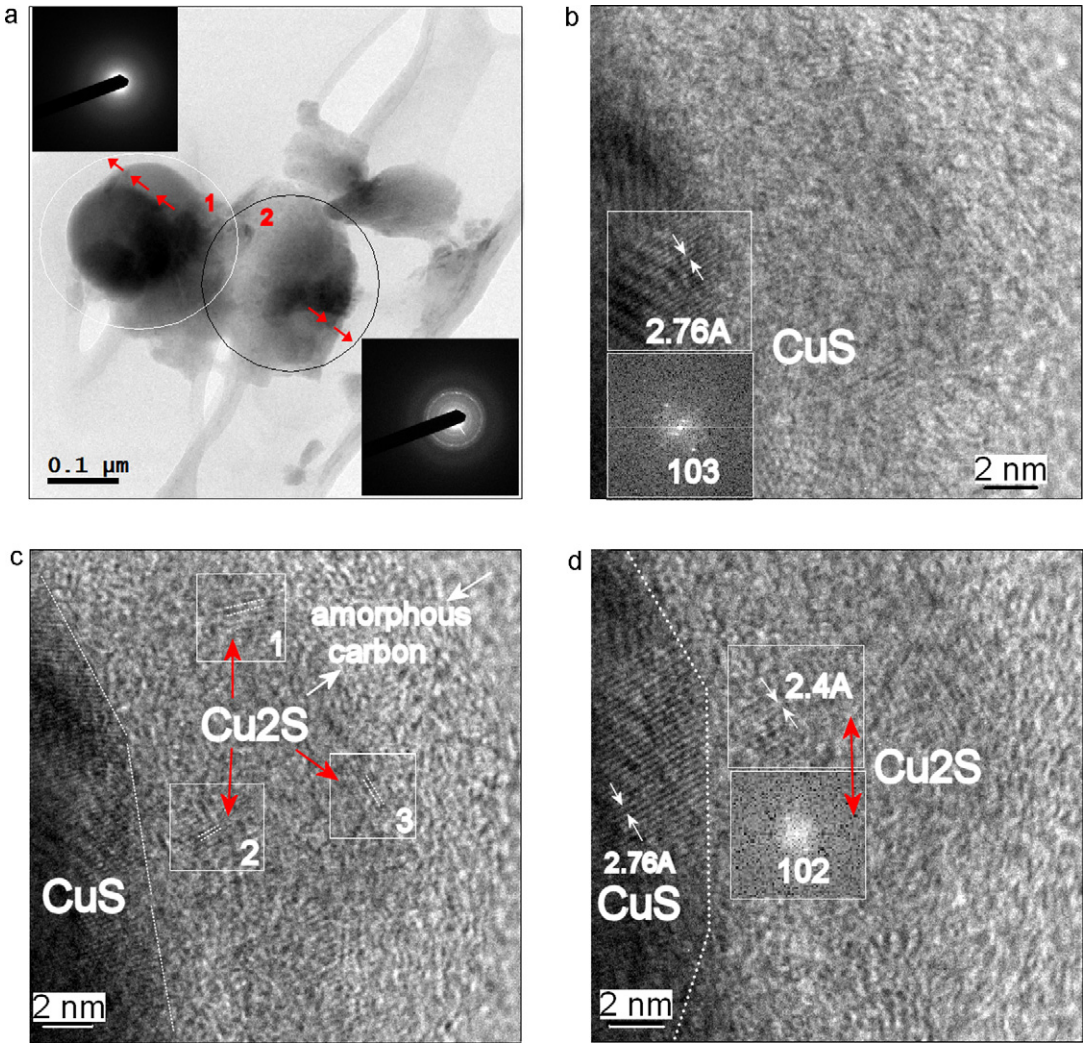

Fig. 8. Electron diffraction and HRTEM images of a nanoregion of coexisting CuS, Cu_2S and carbon, showing adjacent amorphous (1) and nanocrystalline (2) grains-containing bodies (a) together with lattice planes of CuS and Cu_2S with values of corresponding interlayer spacing (b–d) for body 2.

mer and hexagonal carbon. The fast growth of these structures confirms feasible solid state room-temperature reaction between copper and photolytically deposited sulfur, which is not hindered by the co-existence of the photolytic by-products (S/C/H polymer and carbon).

4. Conclusions

Ultraviolet laser-induced photolysis of thiirane allows chemical gas-phase deposition of elemental sulfur (S_6), hexagonal carbon and polythiene. This solid phase interacts with copper at room temperature, allowing growth of amorphous sub-μm-thick and several tens of μm-long filaments that contain Cu_2S and CuS nanograins in their amorphous polythiene- and carbon-containing CuS/Cu_2S bodies. The growth of μm-sized copper sulfides nanostructures shows the occurrence of solid-state reaction between copper and sulfur at room temperature.

Acknowledgement

The authors thank the Grant Agency of the Czech Republic (Grant No. 203/09/0931) for support.

References

[1] S.B. Gadgil, R. Thangaraj, O.P. Agnihotri, Optical properties and solar selectivity of flash-evaporated copper sulphide films, Thin Solid Films 145 (1986) 197–202.
[2] I. Gozdanov, M. Najdoski, Optical and electrical properties of copper sulfide films of variable composition, Solid State Chem. 114 (1995) 469–475.
[3] J.S. Chung, H.J. Sohn, Electrochemical behaviors of CuS as a cathode material for lithium secondary batteries, J. Power Sources 108 (2002) 226–231.
[4] A.A. Sagade, R. Sharma, Copper sulphide (Cu_xS) as an ammonia gas sensor working at room temperature, Sens. Actuators B: Chem. 133 (2008) 135–143.
[5] H. Lee, S.W. Yoon, J. Kim, J. Park, In situ growth of copper sulphide nanocrystals on multiwalled carbon nanotubes and their application as novel solar cell and amperometric glucose sensor, Nano Lett. 7 (2007) 778–784.
[6] Y. Wu, C. Wadia, B. Sadtler, A.P. Alivisatos, Synthesis and photovoltaic copper Cu(I)S sulfide nanocrystals, Nano Lett. 8 (2008) 2551–2555.
[7] X. Jiang, Y. Xie, J. Lu, W. He, L. Zhu, Y. Qian, Preparation and phase transformation of nanocrystalline copper sulfides (Cu_9S_8, Cu_7S_4 and CuS) at low temperature, J. Mater. Chem. 10 (2000) 2193–2196.
[8] G.A. Armantrout, D.E. Miller, K.E. Vindelov, T.G. Brown, Formation of thin Cu_2S (chalcocite) films using reactive sputtering techniques, J. Vac. Sci. Technol. 16 (1979) 212–215.
[9] E. Vanhoecke, M. Burgelman, Reactive sputtering of thin Cu_2S films for application in solar cells, Thin Solid Films 112 (1984) 97–106.
[10] R. Nomura, K. Miyawaki, T. Toyosaki, H. Matsuda, Preparation of copper sulphide thin layers by a single-source MOCVD process, Chem. Vapor Depos. 2 (1996) 174–179.
[11] J. Johansson, J. Kostamo, M. Karppinen, L. Niinistö, Growth of conductive copper sulphide thin films by atomic layer deposition, J. Mater. Chem. 12 (2002) 1022–1026.

[12] W. Zhang, S. Yang, *In situ* fabrication of inorganic nanowire arrays grown from and aligned on metal substrates, Acc. Chem. Res. 42 (2009) 1617–1627.
[13] S. Wang, S. Yang, Growth of crystalline Cu_2S nanowire arrays on copper surface: effect of copper surface structure, reagent gas composition, and reaction temperature, Chem. Mater. 13 (2001) 4794–4799.
[14] Q. Wang, J.-X. Li, G.-D. Li, X.-J. Cao, K.-J. Wang, J.-S. Chen, Formation of CuS nanotube arrays from CuCl nanorods through a gas–solid reaction route, J. Cryst. Growth 299 (2007) 386–392.
[15] C.E. Kliewer, S.L. Soled, S. Miseo, W.R. Kliewer, Ex-situ TEM sulfidation study of supported copper particles, Microsc. Microanal. 12 (2006) 816–817.
[16] H.-X. Zhang, J.-P. Ge, Y.-D. Li, Geometrically kinetic competition mechanism to shape control of digenite nanocrystals with silica vapor in APCVD, J. Phys. Chem. B 110 (2006) 14107–14113.
[17] V. Dusastre, B. Omar, I.P. Parkin, G.A. Shaw, Convenient, room-temperature, amine-assisted routes to metal sulfides, selenides and tellurides, J. Chem. Soc., Dalton Trans. (1997) 3505–3508.
[18] H. Xu, W. Wang, W. Zhu, L. Zhou, Synthesis of octahedral CuS nanocages via a solid–liquid reaction, Nanotechnology 17 (2006) 3649–3654.
[19] W. Wang, L. Ao, Synthesis and characterization of crystalline CuS nanorods prepared via a room temperature one-step, solid reaction, Mater. Chem. Phys. 109 (2008) 77–81.
[20] W. Du, X. Qian, X. Ma, Q. Gong, H. Cao, J. Yin, Shape-controlled synthesis and self-assembly of hexagonal covellite (CuS) nanoplates, Chem. Eur. J. 13 (2007) 3241–3247.
[21] A. Ghezelbash, B. Korgel, Nickel sulphide and copper sulphide nanocrystal synthesis and polymorphism, Langmuir 21 (2005) 9451–9456.
[22] P. Zhang, L. Gao, Copper sulphide flakes and nanodisks, J. Mater. Chem. 13 (2003) 2007–2010.
[23] H. Zhu, J. Wang, Fast synthesis, formation mechanism, and control of thickness of CuS hollow spheres, Inorg. Chem. 48 (2009) 7099–7104.
[24] Q. Lu, F. Gao, D. Zhao, One-step synthesis and assembly of copper sulfide nanoparticles to nanowires, nanotubes, and nanovesicles by a simple organic amine-assisted hydrothermal process, Nano Lett. 2 (2002) 725–728.
[25] C. Wang, K. Tang, Q. Yang, H. Bin, G. Shen, Y. Qian, Synthesis of CuS millimeter-scale tubular crystals, Chem. Lett. (2001) 494–495.
[26] T. Thongtem, A. Phuruangrat, S. Thongtem, Formation of CuS with flower-like, hollow spherical, and tubular structures using the solvothermal-microwave process, Curr. Appl. Phys. 9 (2009) 195–200.
[27] L.A. Isac, A. Duta, A. Kriza, I.A. Enesca, M. Nanu, The growth of CuS thin films by spray pyrolysis, J. Phys. Conf. Ser. 61 (2007) 477–481.
[28] J. Madarász, M. Okuya, S. Kaneko, Preparation of covellite and digenite thin films by an intermittent spray pyrolysis deposition method, J. Eur. Ceram. Soc. 21 (2001) 2113–2116.
[29] L. Wang, C. Xu, D. Zhou, H. Luo, T. Ying, Synthesis of hierarchical CuS flower-like submicrospheres via an ionic liquid-assisted route, Bull. Mater. Sci. 31 (2008) 931–935.
[30] S. Lindroos, A. Arnold, M. Leskelä, Growth of CuS thin films by the successive ionic layer adsorption and reaction method, Appl. Surf. Sci. 158 (2000) 75–80.
[31] X. Liu, G. Xi, Y. Liu, S. Xiong, L. Chai, Y. Qian, Selected synthesis of CuS nanotubes and hollow nanospheres at room temperature, J. Nanosci. Nanotechnol. 7 (2007) 4501–4507.
[32] M. Xin, K. Li, H. Wang, Synthesis of CuS thin films by microwave assisted chemical bath deposition, Appl. Surf. Sci. 256 (2009) 1436–1442.
[33] Y. Zhang, Z.-P. Qiao, X.-M. Chen, Microwave-assisted elemental-direct-reaction route to nanocrystalline copper sulfides Cu_9S_8 and Cu_7S_4, J. Solid State Chem. 167 (2002) 249–253.
[34] R. Blachnik, A. Müller, The formation of Cu_2S from the elements: I. Copper used in form of powders, Thermochim. Acta 361 (2000) 31–52.
[35] R Blachnik, A. Müller, The formation of Cu_2S from the elements: II. Copper used in form of foils, Thermochim. Acta 366 (2001) 47–59.
[36] T Ohtani, M. Motoki, K. Koh, K. Obashima, Synthesis of binary copper chalcogenides by mechanical alloying, Mater. Res. Bull. 30 (1995) 1495–1504.
[37] P. Kalyanaraman, N. Vijayashree, A.G. Samuelson, Low temperature synthesis and interconversions of copper sulphides using acetonitrile, Ind. J. Chem. 33A (1994) 281–283.
[38] K. Tezuka, W.C. Sheets, R. Kurihara, Y.J. Shan, H. Imoto, T.J. Marks, K.R. Poeppelmeier, Synthesis of covellite (CuS) from the elements, Solid State Sci. 9 (2007) 95–99.
[39] O.J. Cain, R.W. Vook, The structure of epitaxial overgrowths of Cu_2S formed on (1 1 1) Cu, Thin Solid Films 58 (1979) 209–213.
[40] J. Pola, A. Ouchi, ArF and KrF laser-induced gas-phase photolysis of selenophene and tellurophene: extrusion of Te and Se and intramolecular 1,3-H shift competing with β-C–C cleavage in C_4H_4 residue, J. Org. Chem. 65 (2000) 2759–2762.
[41] J. Pola, A. Ouchi, UV laser-induced photolysis of diethyl selenium and diethyl tellurium: extrusion of selenium and tellurium via molecular elimination of ethene, J. Organomet. Chem. 629 (2001) 93–96.
[42] A. Ouchi, Z. Bastl, J. Boháček, H. Orita, K. Miyazaki, S. Miyashita, P. Bezdička, J. Pola, Room-temperature reaction between laser chemical vapor deposited selenium and some metals, Chem. Mater. 16 (2004) 3439–3445.
[43] J.H. Scofield, Hartree–Slater subshell photoionization cross-sections at 1254 and 1487 eV, J. Electron Spectrosc. Relat. Phenom. 8 (1976) 129–137.
[44] P. Felder, E.A.J. Wannenmacher, I. Wiedmer, J.R. Huber, Photodissociation of thiirane in a molecular beam at 193 nm, J. Phys. Chem. B 96 (1992) 4470–4477.
[45] F. Qi, O. Sorkhabi, A.G. Suits, S.-H. Chien, W.-K. Li, Photodissociation of ethylene sulfide at 193 nm: a photofragment translational spectroscopy study with VUV synchrotron radiation and ab initio calculations, J. Am. Chem. Soc. 123 (2001) 148–161.
[46] H.L. Kim, S. Satyapal, P. Brewer, R. Bersohn, Photodissociation dynamics of ethylene sulfide at 193 nm, J. Chem. Phys. 91 (1989) 1047–1050.
[47] R. Tomovska, Z. Bastl, V. Vorlíček, K. Vacek, J. Šubrt, Z. Plzák, J. Pola, ArF laser-induced chemical vapor deposition of polythiene films from carbon disulfide, J. Phys. Chem. B 107 (2003) 9793–9801.
[48] B. Meyer, Elemental sulfur, Chem. Rev. 76 (1976) 367–388.
[49] C.G. Munce, G.K. Parker, S.A. Holt, G.A. Hope, A Raman spectroelectrochemical investigation of chemical bath deposited Cu_xS thin films and their modification, Colloids Surf. A: Physicochem. Eng. Aspects 295 (2007) 152–158.
[50] NIST X-ray Photoelectron Spectroscopy Databáze ver. 2.0, NIST Standard Reference Data Program, NIST, Gaithersburg, MD, 1997.
[51] D. Briggs, G. Beamson, High Resolution XPS of Organic Polymers, The Scienta ESCA 300 Database, John Wiley and Sons, Chichester, U.K., 1992.
[52] JCPDS PDF-2 Database, Release 54, International Centre for Diffraction Data, Newton Square, PA, U.S.A., 2004.